Mercury–Thiolate Clusters in Metallothionein. Analysis of Circular Dichroism Spectra of Complexes Formed between α-Metallothionein, Apometallothionein, Zinc Metallothionein, and Cadmium Metallothionein and Hg^{2+}

Wuhua Lu and Martin J. Stillman*

Contribution from the Department of Chemistry, The University of Western Ontario, London, Ontario, Canada N6A 5B7

Received July 7, 1992

Abstract: The mercury binding properties of rabbit liver metallothionein (MT) have been studied at pH 7 using absorption, circular dichroism (CD), and magnetic circular dichroism (MCD) spectroscopies. Optical spectra in the wavelength region to the red of 220 nm in metallothioneins are dominated by the influence of bound metals in two binding site domains on the 3-dimensional structure of the metal binding site. Metal binding involves either isolated MS_n units (where n = 2, 3, or 4 cysteinyl thiolates) or mercury thiolate clusters, part of which can be written as $(RS)_nMSRM(SR)_n$ (n = 1–3), in which up to four cysteinyl (R) sulfurs coordinate the metal in both bridging and terminal positions. Analysis of the CD spectral data for Hg_7–MT formed from apo-MT 2, Zn_7–MT 2, Cd_7–MT 2, and the apo-α, Zn_4–α, and Cd_4–α fragments, identifies complexes with Hg:MT stoichiometric ratios of 4, 7, and 11. Hg_4–α-MT and Hg_7–MT are characterized as involving tetrahedral coordination geometry for mercury. Titrations of Zn_7–MT with Hg^{2+} result in formation first of Hg_7–MT and then of a second species that reaches a maximum at a stoichiometric ratio of between 11 and 12 Hg:MT. Hg_{11}–MT is the sole product when Zn_7–MT is titrated with Hg^{2+} using 50% ethylene glycol as solvent. It is proposed that Hg_{11}–MT involves trigonal coordination of Hg^{2+} by cysteinyl RS^-. Hg^{2+} binding in Cd_7–MT is very much more complicated than with either Zn_7–MT or apo-MT, and no single, well-defined species forms. The CD spectral data measured during formation of Hg_n–MT (n = 7 or 11) at pH > 7 show that the peptide wrapping in the region of the mercury binding site is strongly influenced by the initial presence of the protons in apo-MT, the zinc in Zn_7–MT, and the cadmium in Cd_7–MT. In each case, addition of mercury in excess of 12 Hg:MT opens up the complexes that have formed and quenches the CD spectral intensity, suggesting that a Hg_{20}–MT species exists which involves a random coil with linear X-Hg–(cysS)- coordination, where X is a counterion and each cysteinyl thiolate in the protein binds to one Hg^{2+}, unlike the highly structured Hg_{18}–MT that forms at low pH (Lu, W.; Zelazowski, A. J.; Stillman, M. J. *Inorg. Chem.* **1993**, *32*, 919–926).

Introduction

Metallothioneins (MT) are a class of low molecular weight, cysteine-rich proteins that bind a wide range of metals both in vivo and in vitro. These proteins have been the subject of intensive interest in many branches of the lift sciences over the past three decades.[1-8] Of significance is the 2-domain metal thiolate cluster structure established by NMR studies[7a] for tetrahedrally coordinated cadmium and zinc in Cd,Zn–MT and later by biochemical studies[8] for trigonally coordinated copper(I) in Cu_{12}–MT. Despite similarities between the chemistry of cadmium, zinc, and mercury, the structure of mercury-containing metallothionein is not well established.

Mercury is well known as a highly toxic element that is increasingly accumulating in the environment and entering the food chain of a variety of animals.[9,10] The biological effects of mercury in both its organic and inorganic forms must depend on interactions with amino acids, proteins, enzymes, and nucleic acids. The significance of the accumulation of mercury to the normal function of animals and man can be assessed not only in terms of the absolute quantities of the metal involved but also in terms of the long-term disfunctional consequences of its presence in tissues and organs. The biochemical processes involved in the transport and storage of mercury will include interactions with proteins like albumin and metallothionein, interactions that may be critical to an overall description of the toxicology of mercury.[10]

Jakubowski and co-workers first demonstrated that more than 50% of the Hg^{2+} injected into rats was eluted in a fraction containing compounds now recognized to be metallothionein.[11-16] However, it was only in 1980 that Hg-containing metallothionein

* To whom correspondence should be addressed. FAX: (519) 661-3022. Telephone: (519) 661-3821. E-mail: Stillman@uwo.ca.

(1) Kagi, J. H. R.; Vallee, B. *J. Biol. Chem.* **1960**, *235*, 3460–3465.
(2) Kagi, J. H. R.; Vallee, B. *J. Biol. Chem.* **1961**, *236*, 2435–2542.
(3) (a) Kagi, J. H. R., Nordberg, M., Eds.; *Metallothionein I*; Birkhaeuser: Basel, 1979. (b) Kagi, J. H. R.; Kojima, Y. Eds. *Metallothionein II*; Birkhaeuser: Basel, 1987.
(4) *Metallothioneins*; Stillman, M. J., Shaw, C. F., III, Suzuki, K. T., Eds.; VCH: New York, 1992.
(5) Stillman, M. J. In *Metallothioneins* (Stillman, M. J., Shaw, C. F., III, Suzuki, K. T., Eds.; VCH: New York, 1992; Chapter 4, pp 55–127.
(6) Riordan, J. F., Vallee, B. L., Eds. *Methods in Enzymology, Metallobiochemistry Part B.*; Academic Press Inc.: Orlando, FL, 1991.
(7) (a) Otvos, J. D.; Armitage, I. M. *Proc. Natl. Acad. Sci. U.S.A.* **1980**, *77*, 7094–7098. (b) Boulanger, Y.; Armitage, I. M.; Miklossy, K.-A.; Winge, D. R. *J. Biol. Chem.* **1982**, 257, 13717–13719. (c) Messerle, B. A.; Schaffer, A.; Vasak, M.; Kagi, J. H. R.; Wuthrich, K. *J. Mol. Biol.* **1992**, 225, 433–443.
(8) (a) George, G. N.; Byrd, J.; Winge, D. R. *J. Biol. Chem.* **1988**, *263*, 8199–8203. (b) Nielson, K. B.; Atkin, C. L.; Winge, D. R. *J. Biol. Chem.* **1985**, *260*, 5342–5350. (c) Nielson, K. B.; Winge, D. R. *J. Biol. Chem.* **1985**, *260*, 8698–8701.
(9) Magos, L. In (1984) in *Hazardous Metals in Human Toxicology*; Vercruysse, A., Ed.; Elsevier: Amsterdam, 1984; pp 171–198.
(10) Falchuk, K. H.; Goldwater, L. J.; Vallee, B. L. (1977) In *Chemistry of Mercury*; (McAuliffe, C. A., Ed.); The Macmillan Press Ltd.: London, 1977; pp 261–284.
(11) Jakubowski, M., Piotrowski, J.; Trojamowska, J. K. *Toxicol. Appl. Pharm.* **1970**, *16*, 743–753.
(12) Wisniewska, J. M.; Trojamowska, B.; Piotrowski, J. K.; Jakubuwski, M. *Toxicol. Appl. Pharm.* **1970**, *16*, 754–763.
(13) Piotrowski, J. K.; Trojamowska, B.; Wisniewska, J. M.; Bolanwska, W. *Toxicol. Appl. Pharm.* **1974**, *27*, 11–19.
(14) Ellis, R. W.; Fang, S. F. *Toxicol. Appl. Pharm.* **1971**, *20*, 14–21.
(15) Winge, D. R.; Premakumar, R.; Rajagopalan, K. V. *Arch. Biochem. Biophys.* **1975**, *170*, 242–252.
(16) Zelazowski, A. J.; Piotrowski, J. K. *Biochem. Biophys. Acta* **1980**, *625*, 89–99.

0002-7863/93/1515-3291$04.00/0

was isolated from rat kidneys and the amino acid composition, molar mass, and metal content reported.[16]

Compared with the detailed knowledge about the metal binding stoichiometries and structures adopted by cadmium-, zinc-, and copper-containing metallothioneins,[3-8,17-25] relatively little structural information is available for mercury metallothionein. A number of previous reports have described chemical and spectroscopic properties of mercury-containing metallothioneins.[19-29]

We have previously described the CD, MCD, and absorption spectroscopic properties of Hg_7–MT.[19-21] Johnson and Armitage[26] analyzed the absorption spectra in Hg,Cd–MT formed by adding Hg^{2+} to Cd_7–MT for varying ratios of Hg:Cd:MT and proposed that both linear and tetrahedral mercury(II)–ligand geometries were present with Hg:MT ratios between 5 and 9. Sokolowski et al.[25] reported the binding energy of sulfur $2p_{1/2,3/2}$ in Hg-containing metallothionein from XPS measurements and proposed that dramatic structural changes in the protein occurred upon the complete displacement of cadmium and zinc by mercury in the Hg_8–MT species. We have also reported a XANES study of zinc-, cadmium-, and mercury-containing metallothioneins and have compared these spectra with data measured for a series of inorganic model compounds.[29] In addition to the formation of metalated species based on the M_7–MT and M_{12}–MT structures, which are well established,[4,5,7,8,30-34] we have recently reported the formation of M_{18}–MT species for Ag^+ [34] and Hg^{2+}.[27] Compounds with this stoichiometry must involve a novel 3-dimensional structure.

In this paper, we report a detailed study using the spectroscopic techniques of circular dichroism, magnetic circular dichroism, and absorption of the reactions of mercury with rabbit liver apo-MT, apo-α-MT, Zn_7–MT, Zn_4–α–MT, Cd_7–MT, and Cd_4-α-MT. The CD data unambiguously suggest that two different geometries are involved when Hg^{2+} binds to MT at pH 7. First, Hg_7–MT forms with tetrahedral coordination, and second, Hg_{11}–MT forms with trigonal coordination. The three-dimensional projection of the CD spectral data as a function of Hg:MT stoichiometry emphasizes the sensitivity of the chirality in the metal binding site to the coordination geometry of the bound mercury.

Materials and Methods

Zn_7–MT 2 was isolated from the livers of rabbits injected 10 times with a solution of $ZnSO_4$ (20 mg of zinc/kg body weight) over a 2-week period and purified as described previously.[35] Apo-MT was prepared from Zn–MT by passage down a Sephadex G-25 gel column equilibrated with 0.01 M HCl to remove zinc. The α fragment was prepared from apo-MT as described previously by Winge and Miklossy.[36] Cd_7–MT was reconstructed from apo-MT as previously described.

Protein concentrations were estimated from measurements of -SH groups using 5,5′-dithiobis(nitrobenzoic acid) in 6 M guanidine hydrochloride.[37] Calculations were based on the assumption that there are 20 -SH groups in the whole protein and 11 in the α fragment. For metal-containing metallothioneins, the protein concentrations were confirmed from metal concentrations determined by atomic absorption spectrometry (AAS; Varian 875). The calculations were based on the assumption that there are seven Zn^{2+} or Cd^{2+} per metallothionein.[4] Hg^{2+} concentrations were determined using a method based on a Hg^0 vapor generator.[38a] Metal concentrations were estimated by AAS techniques following addition of Chelex-100 as described previously.[38b]

Circular dichroism spectra were recorded on a Jasco J-500 spectrometer, controlled by an IBM 9001 computer using the program CDSCAN5.[39] Spectra measured from apo-MT and apo-α-MT were taken from separate solutions to which increasing amounts of mercury had been added at pH 2, and the pH was then raised to 7 with Tris buffer. All other titrations were carried out with a single solution of the protein at pH 7. All spectra were measured at room temperature and at pH 7 unless otherwise noted on the figures. Magnetic circular dichroism spectra spectra were recorded on the Jasco J-500 spectrometer with a field of 5.5 T supplied by an Oxford Instruments SM2 magnet. The MCD signal was calibrated by measuring the signal at 510 nm from aqueous $CoSO_4$, $\Delta\epsilon_M = -0.018\ 97$ L mol^{-1} cm^{-1} T^{-1}. Each MCD spectrum reported here has had the zero-field CD spectrum subtracted from it by Spectra Manager. The spectral data were organized and plotted on an HP 7550A plotter with the spectral data base program Spectra Manager[40] for the two-dimensional plots and with program PLOT3D[41] for the three-dimensional plots. Contour lines represent steps 5% of the intensity span shown and were calculated from the 3-dimensional projections. The contour diagrams provide accurate values for peak maxima as a function of Hg:MT molar ratios.

Results

Unlike reactions of Cd^{2+} with metallothionein, which are completed immediately after addition of Cd^{2+} to the protein solution, reactions between Hg^{2+} and metallothionein need 20 min to reach completion at room temperature. Each of the spectra reported in this paper was measured following enough time to allow the reaction to proceed to completion. We use the term isodichroic to indicate the spectral feature observed in the CD or MCD spectrum for two interconverting species. The presence of sharp isodichroic points is strong evidence that only to species are involved.

Hg^{2+} Binding to apo-MT. Figure 1 shows CD and MCD spectra recorded for a series of separate solutions of rabbit liver apo-MT 2 with Hg^{2+} at room temperature. The 3-dimensional projection in Figure 2 allows the strong dependence of the Hg:MT ratio on the CD spectral envelope to be seen. Significant CD spectral effects include (i) nonisodichroic band formation at 240 and 275

(17) Stillman, M. J.; Cai, W.; Zelazowski, A. J. *J. Biol. Chem.* **1987**, *262*, 4358–4548.
(18) Shaw, C. F.; Stillman, M. J.; Suzuki, K. T. In *Metallothioneins*; Stillman, M. J., Shaw, C. F., III, Suzuki, K. T., Eds.; VCH: New York, 1992; Chapter 1, pp 1–13.
(19) Stillman, M. J.; Law, A. Y. C.; Szymanska, J. A. (1983) In *Chemical Toxicology and Clinical Chemistry of Metals*; Brown, S. S., Savory, J., Eds.; Harcourt Brace: London, 1983; pp 271–274.
(20) Szymanska, J. A.; Law, A. Y. C.; Zelazowski, A. J.; Stillman, M. J. *Inorg. Chim. Acta* **1983**, *79*, 123–124.
(21) Szymanska, J. A.; Zelazowski, A. J.; Stillman, M. J. *Biochem. Biophys. Res. Commun.* **1983**, *115*, 167–173.
(22) Nielson, K. B.; Atkin, C. L.; Winge, D. R. *J. Biol. Chem.* **1985**, *260*, 5342–5350.
(23) Vasak, M.; Kagi, J. H. R. (1983) In *Metal Ions in Biological Systems*; Sigel, H., Ed.; Marcel Dekker: New York, 1985; pp 213–273.
(24) Vasak, M.; Kagi, J. H. R.; Hill, H. A. O. *Biochemistry* **1981**, *20*, 2852–2856.
(25) Sokolowski, G., Pilz, W.; Weser, U. *FEBS Lett.* **1974**, *48*, 222–225.
(26) Johnson, B. A.; Armitage, I. M. *Inorg. Chem.* **1987**, *26*, 3139–3145.
(27) (a) Cai, W.; Stillman, M. J. *J. Am. Chem. Soc.* **1988**, *110*, 7872–7873. (b) Lu, W.; Zelazowski, A. J.; Stillman, M. J. *Inorg. Chem.* **1993**, *32*, 919–926.
(28) Willner, H.; Bernhard, W. R.; Kagi, J. H. R. In *Metallothioneins*; Stillman, M. J., Shaw, C. F., III, Suzuki, K. T., Eds.; VCH: New York, 1992; Chapter 5, pp 128–143.
(29) Lu, W.; Kasrai, M.; Tan, K. H.; Bancroft, G. M.; Stillman, M. J. *Inorg. Chem.* **1990**, *29*, 2561–2563.
(30) Furey, W. F.; Robbins, A. F.; Clancy, L. L.; Winge, D. R.; Wang, B. C.; Stout, C. D. *Science* **1986**, *231*, 704–710.
(31) (a) Robbins, A. H.; McRee, D. E.; Willamson, M.; Collett, S. A.; Xuong, N. H.; Furey, W. F.; Wang, B. C.; Stout, C. D. *J. Mol. Biol.* **1991**, *221*, 1269–1293. (b) Robbins, A. H.; Stout, C. D. In *Metallothioneins*; Stillman, M. J., Shaw, C. F., III, Suzuki, K. T., Eds.; VCH: New York, 1992; Chapter 3, pp 31–54.
(32) Stillman, M. J.; Gasyna, Z. In *Methods in Enzymology, Metallobiochemistry Part B*; Riordan, J. F., Vallee, B. L., Eds.; Academic Press Inc.: Orlando, FL, 1991; Vol. 205, Chapter 62, pp 540–555.
(33) Green, A. R.; Presta, P. A.; Gasyna, Z.; Stillman, M. J., unpublished results. (b) Presta, P. A.; Green, A. R.; Zelazowski, A. J.; Stillman, M. J., unpublished results.
(34) (a) Zelazowski, A. J.; Gasyna, Z.; Stillman, M. J. *J. Biol. Chem.* **1989**, *264*, 17091–17099. (b) Zelazowski, A. J.; Stillman, M. J. *Inorg. Chem.* **1992**, *31*, 3363–3370.
(35) Zelazowski, A. J.; Szymanska, J. A.; Witas, H. *Prep. Biochem.* **1980**, *10*, 495–505.
(36) Winge, D. R.; Miklossy, K. *J. Biol. Chem.* **1982**, *257*, 3471–3476.
(37) Ellman, G. L. *Arch. Biochem. Biophys.* **1959**, *82*, 70–77.
(38) (a) Lu, W.; Stillman, M. J. In *Metallothioneins*; Stillman, M. J., Shaw, C. F., III, Suzuki, K. T., Eds.; VCH: New York, 1992; Chapter 8, pp 186–194. (b) Cai, W.; Stillman, M. J. *Inorg. Chim. Acta* **1988**, *152*, 111–115.
(39) Gasyna, Z.; Browett, W. R.; Nyokong, T.; Kitchenham, B.; Stillman, M. J. *Chemom. Intell. Lab. Syst.* **1989**, *5*, 233–246.
(40) Browett, W. R.; Stillman, M. J. *Comput. Chem.* **1987**, *11*, 73–80.
(41) Gasyna, Z.; Stillman, M. J., unpublished program.

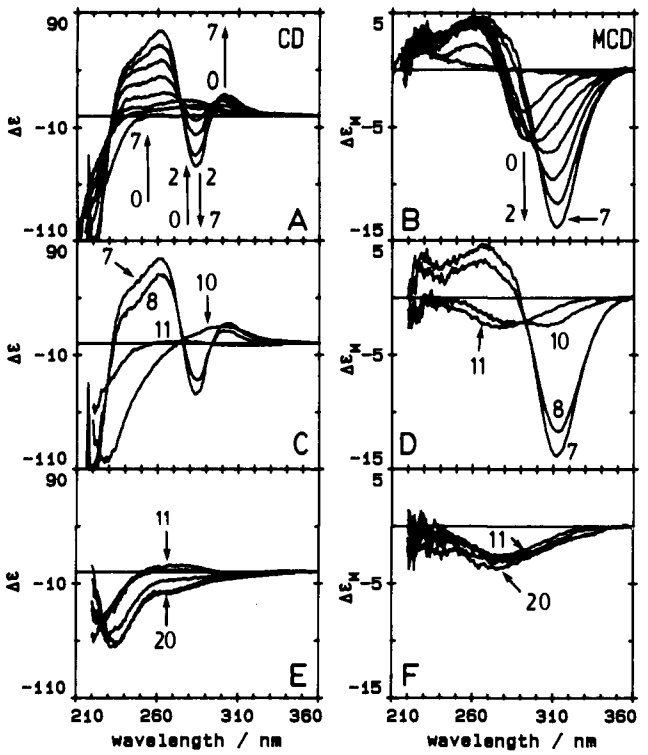

Figure 1. CD and MCD spectra recorded for a series of separate solutions of rabbit liver apo-MT 2 with increasing molar ratio of Hg^{2+}:MT. Top row: CD (A) and MCD (B) spectra with 0, 1.0, 2.0, 3.0, 4.0, 5.0, 6.0, and 7.0 Hg^{2+}. Middle row: CD (C) and MCD (D) spectra with 7.0, 8.0, 10.0, and 11.0 Hg^{2+}. Bottom row: CD (E) and MCD (F) spectra with 11.0, 12.0, 15.0, 19.0, and 20.0 Hg^{2+}. THe MCD units of $\Delta\epsilon_M$ are L mol^{-1} cm^{-1} T^{-1}; the corresponding zero-field CD spectrum has been subtracted from the field-on spectrum; field was 5.5 T. The arrows show either the direction of change in intensity for a range of Hg:MT values or spectra for a single solution. Conditions: separate samples, 10 μM protein.

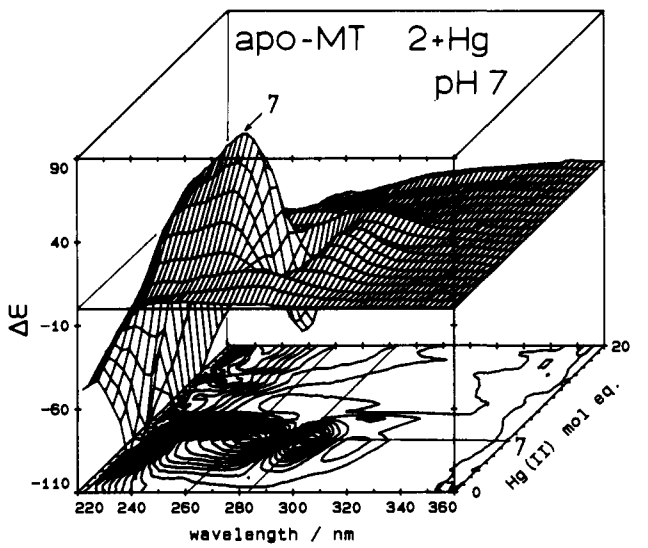

Figure 2. 3-D projection plot of the CD spectra recorded for a series of separate solutions of rabbit liver apo-MT 2 with increasing molar ratio of Hg^{2+}:MT. The Hg:MT molar ratio spans 0–20. The 7 identifies the maximum signal intensity observed for Hg:MT = 7. The z axis is plotted in units of the Hg^{2+} added to each of the solutions of apo-MT. The grid lines added to the contour diagram are drawn for an Hg^{2+} molar ratio of 7 and indicate the following wavelengths: 260 and 284 nm. Conditions: separate samples, 10 μM protein.

nm for the first 2 Hg^{2+} added, (ii) isodichroic (at 273 and 293 nm) band intensification (at 261, 283, and 303 nm) from 2 to 7 Hg^{2+}, (iii) band maxima formation at exactly 7 Hg:MT, (iv)

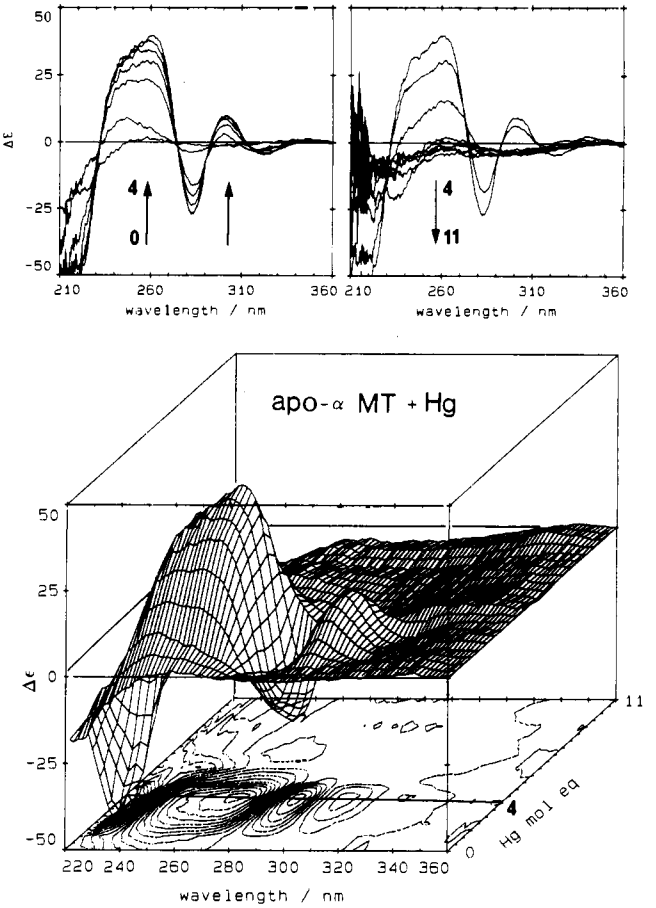

Figure 3. CD spectra recorded for a series of separate solutions of rabbit liver apo-α-MT 2 with increasing molar ratio of Hg^{2+}:MT. Top left: (A) CD spectra recorded with 0, 1.0, 2.0, 2.5, 3.0, 3.5, and 4.0 Hg^{2+}; the spectral intensity increases over this range with isodichroic points at 274 and 292 nm. Top right: (B) CD spectra recorded with 4.0, 4.5, 5.0, 6.0, 7.0, 8.0, 9.0, 10.0, and 11.0 Hg^{2+}; the spectral intensity collapses steeply as a function of the Hg:MT ratio with isodichroic points at 273 and 290 nm. 3-D projection plot. CD data for solutions of apo-α MT 2 with Hg:MT from 0 to 11. The z axis is plotted in units of the Hg^{2+} added to each of the solutions of apo-α-MT 2. The 4 marks the maximum spectral intensity. The grid lines added to the contour diagram are drawn for Hg^{2+} molar ratio of 4 and indicate 260, 283, and 302 nm. Conditions: separate samples, 10 μM protein.

growth of a low-intensity band at 300 nm with 10 Hg^{2+} added, before, finally, (v) isodichroic (274 nm) collapse of the CD intensity with Hg:MT > 11. Even though there is no CD spectral intensity at Hg:MT mole ratios greater than 12, the Hg^{2+} must still be bound to the protein up to Hg:MT of 20. Only at this high molar ratio is free Hg^{2+} measured. The lack of a CD spectral band implies a lack of 3-D structure that exhibits a chiral structure, not that the Hg^{2+} is not binding. The MCD spectral changes arise from quite different intensity mechanisms[5] and can be summarized as (i) 290-nm band formation for 1 and 2 Hg^{2+}, (ii) intensification of bands at 268 (+) and 311 nm (–) with 7 Hg^{2+}, and finally, (iii) isodichroic (at 294 nm) collapse of the intensity from 7 to 11 Hg^{2+}. We discuss the bandshape observed in the MCD spectrum below.

Hg^{2+} Binding to apo-α-MT. Figure 3 shows a series of CD spectra recorded for separate solutions of apo-α-MT 2 with an increasing molar ratio of Hg:MT. Significant spectroscopic changes are (i) isodichroic (274 and 292 nm) growth of a spectral envelope with maxima at 261, 283, 300, and 322 nm (it is important to note that the whole spectral envelope exhibits the same dependence on the Hg:MT ratio) and (ii) isodichroic (at 273 and 290 nm) collapse of the CD intensity with Hg:MT > 4. The band maxima at exactly 4 Hg^{2+} and the sharp isodichroic points

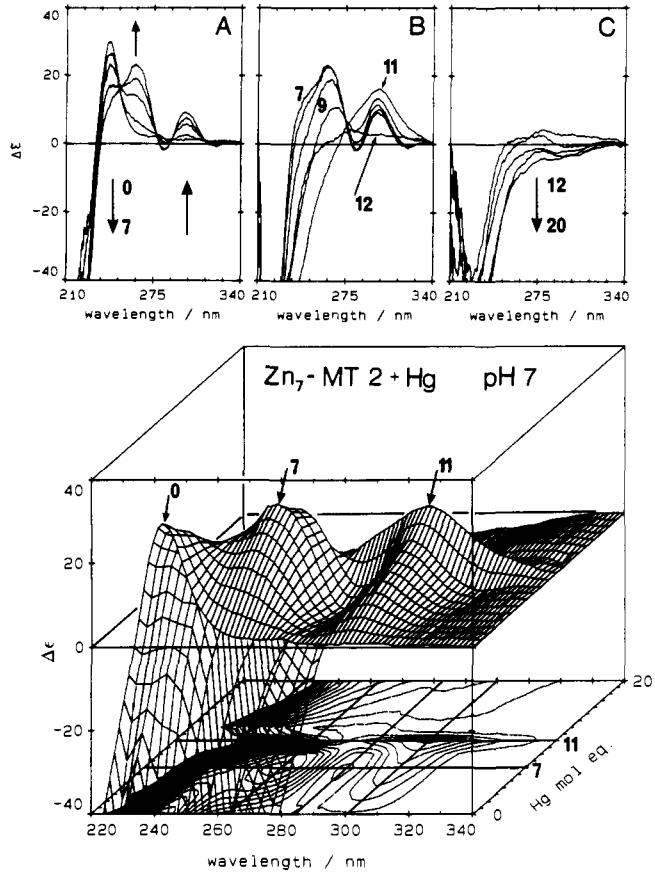

Figure 4. CD spectra recorded during a titration of a single sample of rabbit liver Zn_7–MT 2 with Hg^{2+}. (A) CD spectra with 0, 1.0, 3.0, 5.0, and 7.0 Hg^{2+}; the spectral intensity increases in magnitude at 262, 282, and 297 nm, with isodichroic points at 250, 278, and 289 nm. (B) CD spectra with 7.0, 8.0, 9.0, 10.0, 11.0, and 12.0 Hg^{2+}; the spectral intensity decreases in the 260-nm region and increases in the 300-nm region up to Hg:MT = 11; the CD spectrum for Hg:MT = 12 is featureless. (C) CD spectra with 13.0, 15.0, 17.0, 19.0, and 20.0 Hg^{2+}. 3-D projection plot. The band labeled 0 represents the CD spectrum of Zn_7–MT, and the 7 and 11 labels mark maxima in the CD spectra. The z axis is plotted in units of the Hg^{2+} added to the solution of Zn_7–MT 2. The grid lines added to the contour diagram are drawn for Hg^{2+} molar ratios of 7 and 11 and indicate 285 and 300 nm. Conditions: single sample, 10 μM protein, H_2O as solvent.

for this titration indicate that the Hg_4–α-MT is the only species being formed between 0 and 4 Hg^{2+}. The peak-to-trough CD intensity for Hg_4–α-MT is about 57% that of Hg_7–MT, a value that represents the relative Hg^{2+} loading in Hg_4–α-MT compared with Hg_7–MT. Again, no free Hg^{2+} will exist up to the 11 Hg:MT point (where each of the 11 cysteinyl thiolates will be bound to a single Hg^{2+}). Although the broad band with 1 or 2 Hg^{2+} that was seen with apo-MT is absent, the CD spectrum measured with 1 Hg^{2+} is not the same as the spectrum recorded for Hg_4–α-MT, exhibiting a maximum at 240 rather than at 260 nm.

Hg^{2+} Binding to Zn_7–MT. Figures 4 and 5 show the much more complicated set of absorption, CD, and MCD spectra recorded during a titration of single samples of Zn_7–MT 2 in H_2O with Hg^{2+}. The spectral changes are summarized in Table I. Three stages can be seen in the titration, at Hg:MT molar ratios of (i) 0–8 (Figures 4A, 5A, 5B), (ii) 8–12 (Figures 4B, 5C, 5D), and (iii) 12–20 (Figures 4C, 5E).

There are important differences between the MCD spectra recorded during the reaction of Hg^{2+} with Zn_7–MT (Figures 5A, 5B) and apo-MT (Figures 1B, 1C). First, and most significantly, the MCD signal intensity from the Hg–SR chromophore measured during the titration of Zn_7–MT with Hg^{2+} grows in intensity continuously at 311 nm (–) as the molar ratio of Hg:MT increases to 7, and the band center does not red-shift. There is no indication

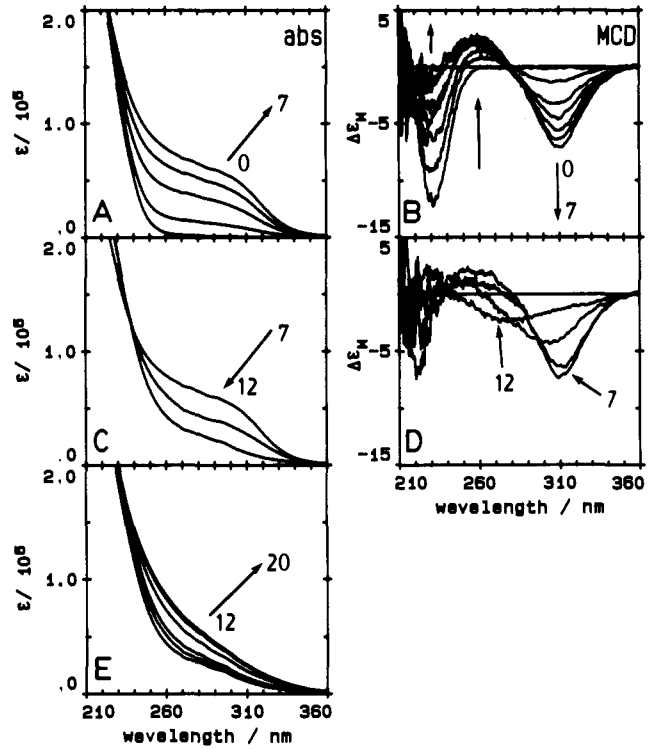

Figure 5. Adsoprtion and MCD spectra recorded during a titration of rabbit liver Zn_7–MT 2 with Hg^{2+}. Absorption spectra. (A) Spectra with 0, 1.0, 3.0, 5.0, and 7.0 Hg^{2+}. (C) Spectra with 7.0, 9.0, and 12.0 Hg^{2+}. (E) Spectra with 12.0, 13.0, 14.0, 17.0, 19.0, and 20.0 Hg^{2+}. MCD spectra. (B) Spectra with 0, 1.1, 2.7, 3.7, 4.8, 5.8, and 7.0 Hg^{2+}. (D) Spectra with 7.00, 8.5, 10.1, and 11.7 Hg^{2+}. The units of $\Delta\epsilon_M$ are L mol^{-1} cm^{-1} T^{-1}; the corresponding zero-field CD spectrum has been subtracted from the field-on spectrum; field was 5.5 T. Conditions: single sample, 10 μM protein, H_2O as solvent.

Table I. Changes in Absorption, CD, and MCD Spectra as Mercury is Added to Zn_7–MT 2 at pH 7 (Figures 4 and 5)

molar ratio Hg:MT	spectral changes observed
0–7	absorption: linear increase in absorption in the 260–310-nm region CD: initial 242-nm (+) band of Zn_7-MT decreases in intensity with isodichroic points at 250, 278, and 289 nm; bands at 262 (+), 285 (–), and 300 nm (+) intensify to amaximum at 7 Hg(II) MCD; increase in band intensity at 260 and 310 nm (–), with no red shift
7–12	absorption: decrease in 290-nm region with a blue shift toward maxima at 270 and 290 nm CD: bands at 240 (+) and 262 nm (+) decrease in intensity with a new isodichroic point at 275 nm; 300-nm (+) band broadens and intensifies at Hg(II) > 9; at the 11 Hg(II) point, the 300-nm (+) band replaces all other spectral features MCD; isodichroic decrease in intensity at 310 nm from 7–11 Hg(II); a nonidosidchroic blue shift of the band center to 270 nm
12–20	absorption: slight increase at 290 nm to a maximum for 20 Hg(II) CD: 300-nm (+) band steeply decreases in intensity at 12 Hg(II)

of the species characterized by the 295-nm (–) band observed at low (1–2) Hg:MT molar ratios with apo-MT. Second, the band at 220 nm arising from the Zn–SR chromophore decreases in intensity to reach 0 at the 7 Hg^{2+} point, further confirming the stoichiometric replacement of Zn^{2+} by Hg^{2+}. Third, the crossover points with 0 intensity are different. For apo-MT with Hg^{2+}, the crossover wavelength with 1 to 2 Hg^{2+} is at 276 nm, and then a

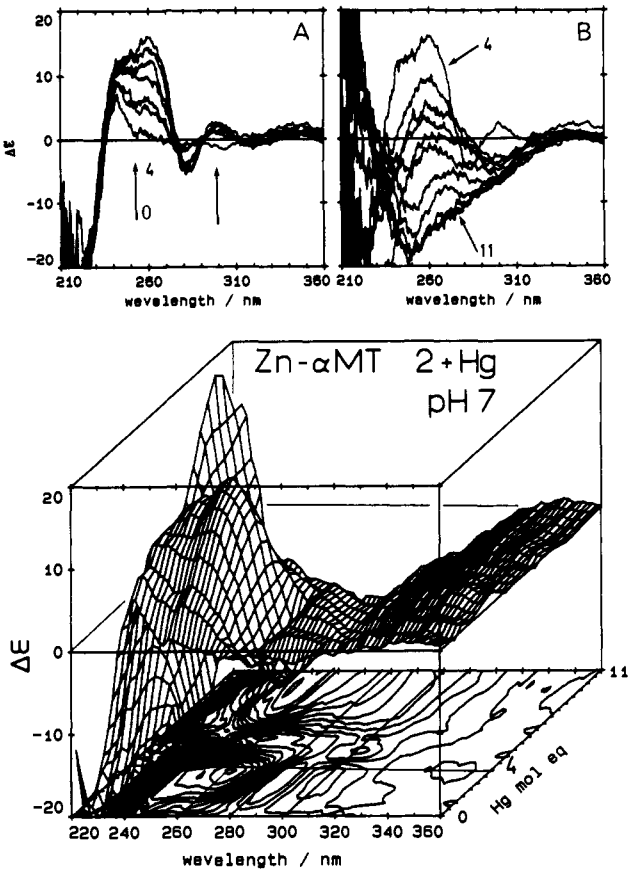

Figure 6. CD spectra recorded during a titration of rabbit liver Zn_4–α-MT 2 with Hg^{2+}. (A) Spectra with 0, 0.5, 1.1, 1.6, 2.2, 2.7, and 3.2 Hg^{2+}. (B) Spectra with 3.2, 4.3, 4.9, 5.4, 6.0, 6.5, 7.0, 7.6, 8.7, 9.7, and 10.8 Hg^{2+}. 3-D plot. The z axis is plotted in units of the Hg^{2+} added to the solution of Zn–α-MT 2. The grid lines added to the contour diagram are drawn for an Hg^{2+} molar ratio of 3.5 and indicate 260, 280, and 300 nm. Conditions: single sample, 10 μM protein, H_2O as solvent, room temperature.

gradual red shift to 291 nm occurs with 3 to 7 Hg^{2+}. For Zn_7–MT with Hg^{2+}, the crossover wavelength remains at 276 nm for the whole titration. Finally, fourth, the 310-nm MCD band intensity from Hg–MT formed from Zn–MT with 7 Hg^{2+} is only half as intense as that for Zn_7–MT formed from apo-MT.

The data show, therefore, that three distinct species are formed when up to 20 Hg^{2+} are added to Zn_7–MT. Of greatest importance is the species that forms with a well-defined 3-dimensional structure at Hg:MT ratios of 11.

Hg^{2+} Binding to Zn_4–α–MT. Figure 6 shows CD spectra recorded during a titration of a 10 μM solution of Zn–α-MT 2 with Hg^{2+}. The spectroscopic changes include (i) isodichroic (276 and 290 nm) intensification (242 (+), 260 (+), 282 (–), 300 (+), and 320 (–)) between 1 and 4 Hg^{2+} and (ii) complete nonisodichroic loss of the resolved CD spectral intensity with >4 Hg^{2+}. Although the spectral data are much noisier than we find when Hg^{2+} is added to either apo-MT or Zn_7-MT or Zn_7–MT, the sharp isodichroic points and the growth in band intensity from 1.1 to 2.2 to 3.2 Hg^{2+} (the sharp collapse of the signal with Hg:MT > 4 means that when there is some loss of metallothionein it is difficult to measure the saturated signal) show that a single Hg_4–α-MT species forms in this titration. Although the band envelope is better resolvled than the CD spectrum measured for Hg_7–MT formed from Zn_7–MT, exactly the same band maxima are found. The nonisodichroic behavior of the spectral data in Figure 6B suggests that with Hg:MT > 4 the cluster structure immediately opens and a new complex begins to form with a maximum near Hg:MT = 7. A similar effect has been observed for Ag^+ binding to Zn_4–α MT,[34b]

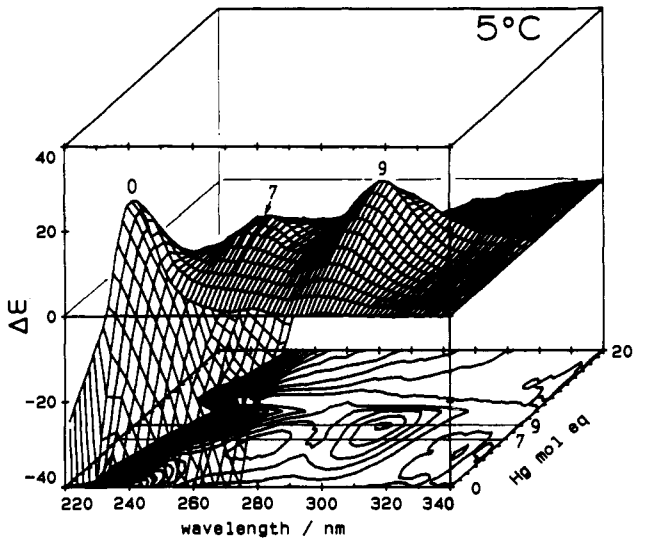

Figure 7. CD spectra recorded during a titration of rabbit liver Zn_7–MT 2 with Hg^{2+} at 5 °C. The z axis is plotted in units of the Hg^{2+} added to the solution of Zn_7–MT 2. The grid lines added to the contour diagram are drawn for Hg^{2+} molar ratios of 7 and 9. The band labeled 0 represents the CD spectrum of Zn_7–MT, and 7 and 9 labels mark maxima in the CD spectra. Conditions: single sample, 10 μM protein, H_2O as solvent.

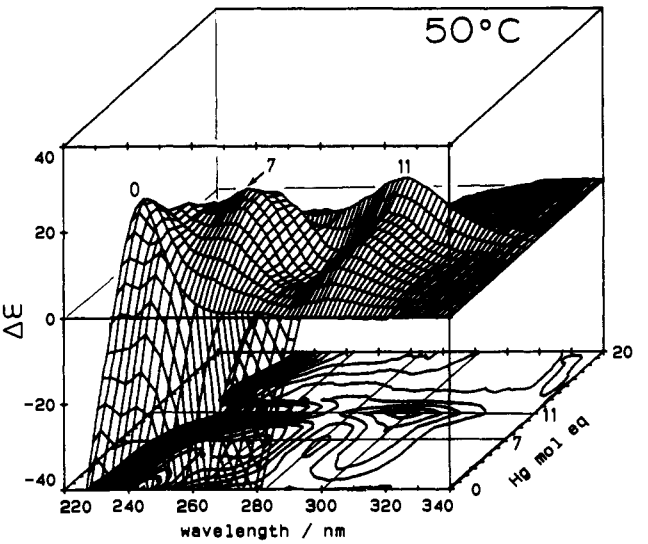

Figure 8. CD spectra recorded during a titration of rabbit liver Zn_7–MT 2 with Hg^{2+} at 50 °C. The z axis is plotted in units of the Hg^{2+} added to the solution of Zn_7–MT 2. The grid lines added to the contour diagram are drawn for Hg^{2+} molar ratios of 7 and 11, and indicate 262, 285, and 300 nm. The band labeled 0 represents the CD spectrum of Zn_7–MT, and 7 and 11 labels mark maxima in the CD spectra. Conditions: single sample, 10 μM protein, H_2O as solvent.

Temperature Effects on Hg^{2+} Binding to Zn–MT. Figures 7–9 show a series of 3-dimensional projection plots of CD spectra recorded during titrations of 10 μM solutions of Zn_7–MT 2 with Hg^{2+} at 5 °C (Figure 7), 23 °C (Figure 4), 50 °C (Figure 8), and 70 °C (Figure 9). We measured a series of CD spectra at a range of temperatures to examine the requirements for peptide refolding following exchange of metals. At 5 °C (Figure 7), the loss of the 240-nm band of the Zn–SR chromophore indicates that stoichiometric displacement of the Zn^{2+} takes place. Intensification of the characteristic Hg–SR band at 261 but not at 280 nm (–) only poorly develops when 7 Hg^{2+} have been added. The broad 302–nm (+) band reaches a maximum at 9 Hg^{2+} rather than at 11 Hg^{2+}. The 300-nm (+) band intensity decreases to 0 at 12 Hg^{2+}, as observed earlier. At 50 °C (Figure 8), the CD bands are almost the same as the CD spectra recorded at room temperature (Figure 4) except that the 262-nm (+)/282-

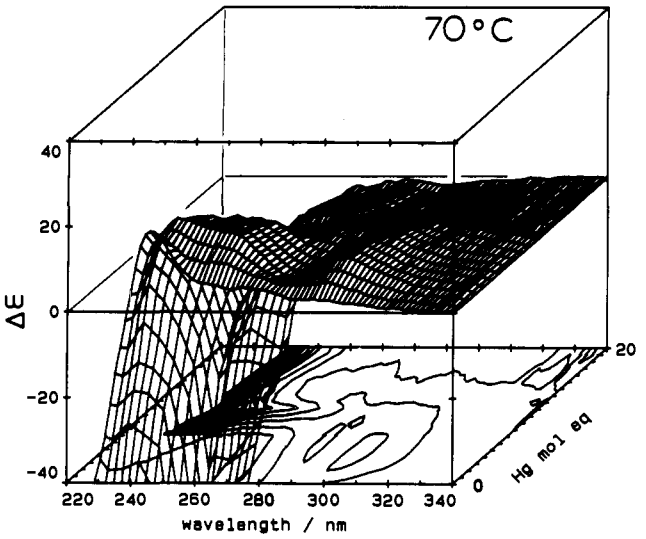

Figure 9. CD spectra recorded during a titration of rabbit liver Zn_7–MT 2 with Hg^{2+} at 70 °C. The z axis is plotted in units of the Hg^{2+} added to the solution of Zn_7–MT 2. Conditions: 10 μM protein, H_2O as solvent.

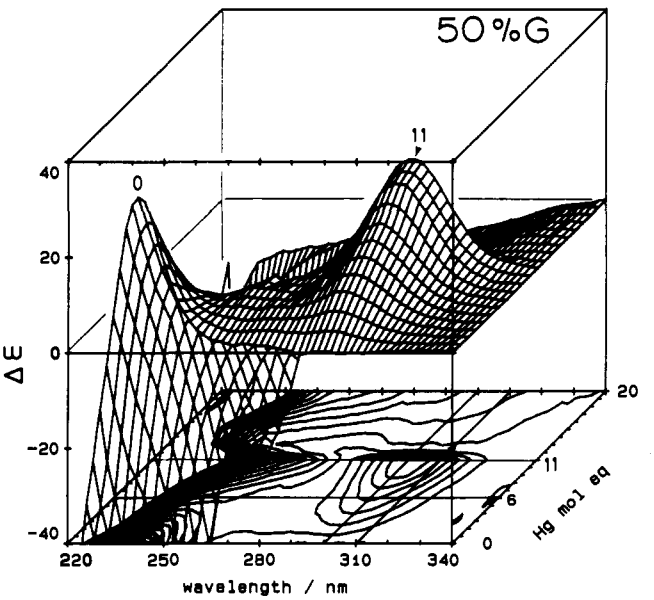

Figure 10. Effect on the CD spectra recorded during titrations of rabbit liver Zn_7–MT 2 with Hg^{2+} of using 50% ethylene glycol as solvent. The z axis is plotted in units of the Hg^{2+} added to the solution of Zn_7–MT 2. The grid lines added to the contour diagram are drawn for Hg^{2+} molar ratios of 6 and 11 and indicate 300 nm. Conditions: single sample, 10 μM protein, 50% ethylene glycol as solvent.

nm (–) band sequence is less well resolved than at room temperature. The speciation that results in the intensity at 300 nm is more clearly resolved, with a sharp increase in intensity between 9 and 11 Hg. The development of bands at 262, 282, and 300 nm between 3 and 6 Hg^{2+} clearly arises from the same species. The broader band that intensifies between 9 and 11 Hg^{2+} must arise from a different species. The titration carried out at 70 °C (Figure 9) shows only minimal CD intensity.

Solvent Effects on Hg^{2+} Binding to Zn_7–MT. A mixture of 50% aqueous ethylene glycol was used as a solvent to investigate effects of changes in solvent polarity, Figure 10. The effect of using ethylene glycol is very dramatic as only the species responsible for the 300-nm band, which is at a maximum at 11 Hg:MT, forms, while the CD envelope characteristic of Zn_7–MT steeply diminishes in intensity between 1 and 6 Hg^{2+}. The lack of an envelope characteristic of Hg_7–MT at 261, 283, and 303 nm means that we can observe the complete development of the spectrum of Hg_{11}–MT.

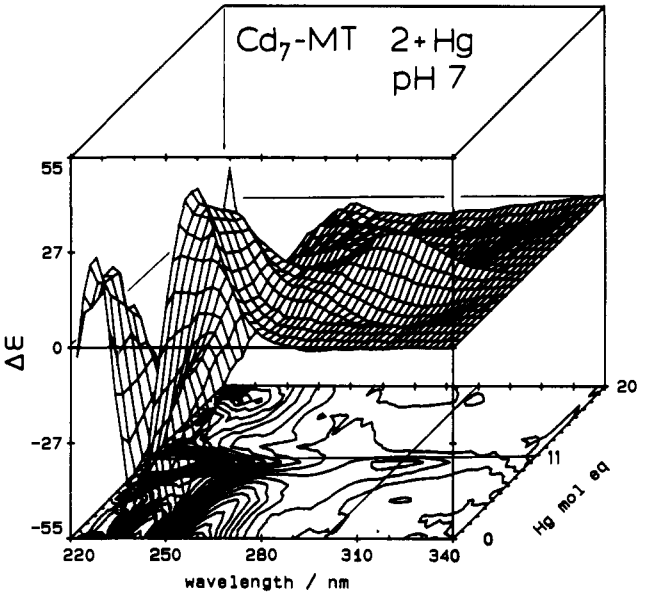

Figure 11. 3-D plot of CD spectra recorded during a titration of rabbit liver Cd_7–MT 2 with Hg^{2+}. The z axis is plotted in units of the Hg^{2+} added to the solution of Cd_7–MT 2. The grid lines added to the contour diagram are drawn for an Hg^{2+} molar ratio of 11 and indicate 300 nm. Conditions: single sample, 10 μM protein, H_2O as solvent.

Hg^{2+} Binding to Cd_7–MT. Figure 11 shows CD spectra recorded during a titration of a 10 μM solution of Cd_7–MT with Hg^{2+}. MCD spectra recorded during this titration (not shown) display a sequence of spectral envelopes, which resemble those of Cd–MT,[15] that appear simply to diminish in intensity as the titration proceeds. The CD spectral changes are (i) gradual loss of the CD spectrum of Cd_7–MT between 1 and 8 Hg^{2+}, (ii) growth of a weak band at 300 nm up to a maximum at 11 Hg^{2+}, and (iii) the collapse of all CD intensity with $Hg^{2+} > 11$. When the spectral data in Figure 11 are compared with the data shown in Figure 4 for Zn–MT, it is clear that only a very small stoichiometric fraction of the Hg_7–MT and Hg_{11}–MT species forms. The same characteristic contours can be seen in Figures 4 and 11. The 257-nm (+) CD band of Cd–MT masks the intensification of the 265-nm (+) band of Hg–MT, but the red shift seen in the contour diagram of Figure 11 and the broadness in the positive CD band near 262 nm both point to the presence of a new band that has a maximum intensity at 7 Hg^{2+}. The species responsible for this band is replaced by another species that is identified by the band at 300 nm.

Hg^{2+} Binding to Cd_4–α-MT. Figure 12 shows CD and absorption spectra recorded during a titration of a 10 μM solution of Cd_4–α-MT with Hg^{2+} at room temperature. Even though the absorption spectra indicate that Cd^{2+} is replaced by Hg^{2+} (decrease in the absorbance at 250 nm and increase at 300 nm from 1 to 4 Hg^{2+}), the CD spectra shown in Figure 12 do not resemble those measured for apo–α-MT with Hg^{2+}, for Zn_4–α-MT with Hg^{2+}, or, surprisingly, for the titration of Cd_7–MT with Hg^{2+}. Cd_4–α-MT exhibits a well-resolved derivative-shaped CD spectrum[17] with band maxima at 224 (+), 240 (–), and 262 (+) nm; these bands are replaced isodichroically (at 250 nm) by a spectrum that exhibits one resolved band at 238 nm. These data indicate that formation of a mercury thiolate cluster structure is completely inhibited by the presence of the Cd^{2+}.

Discussion

The CD spectrum in the wavelength region to the red of 220 nm in metallothioneins is dominated by the influence of the metals on the 3-dimensional structure of the peptide chain that forms the metal binding site.[5,17] The spectral intensity in this region arises from ligand-to-metal charge transfer,[3,4] The transition

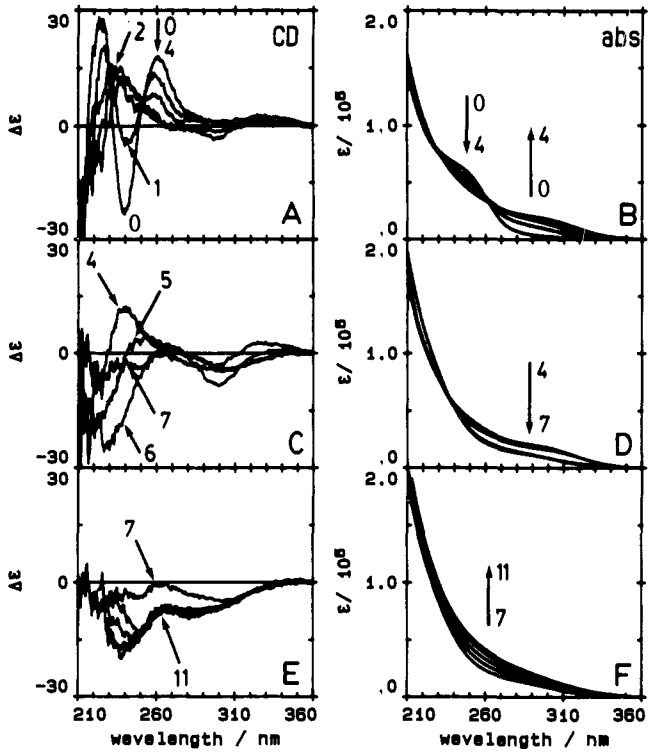

Figure 12. CD and absorption spectra recorded during a titration of rabbit liver Cd_4-α-MT 2 with Hg^{2+}. (A) and (B) Show spectra with 0, 1.0, 2.0, 3.0, and 4.0 Hg^{2+}. (C) and (D) Show spectra with 4.0, 5.0, 6.0, and 7.0 Hg^{2+}. (E) and (F) Show spectra with 7.0, 8.0, 9.0, 10.0, and 11.0 Hg^{2+}. Conditions: single sample, 10 μM protein, H_2O as solvent.

energies for Zn-(cysS)-, Cd-(cysS)-, and Hg-(cysS)- follow a general red shift.[4,5,17,19,23,24,42] However, while Jørgensen's analysis[42] describes the energy of the lowest energy band, there are for Hg_7–MT clearly several bands between 220 and 400 nm. These bands can arise from the presence of different geometries (linear, trigonal, and tetrahedral) around the Hg^{2+} or from the contribution of both terminal and bridging thiolate groups in the coordination sphere of the Hg^{2+}.

Structures for the metal-saturated Cd_7–MT and Zn_7–MT involve M_3S_9 and M_4S_{11} units with both bridging and terminal sulfurs tetrahedrally coordinating the metals,[3,4,7,31] However, while Cd^{2+} appears to be able to replace Zn^{2+} isomorphously, retaining the tetrahedral geometry for each CdS_4 unit,[17] analysis of absorption spectral data by Johnson and Armitage[26] led to the suggestion that Hg^{2+} binding to Cd_7–MT is much more complicated than this, with at least two coordination geometries being involved. This is a significant finding because future structural studies using NMR spectroscopy, XANES, EXAFS, or X-ray diffraction from a crystal will require the homogeneity of the metal binding sites to be known before spectroscopic analysis can be carried out. Therefore, prior studies must address the specificity of the binding geometry to each metal. Do Cd^{2+}, Zn^{2+}, and Hg^{2+} only bind to MT in tetrahedrally coordinated sites? Do Cu^+ and Ag^+ only bind to MT in trigonally coordinated sites?

The CD spectra described here for titrations of Hg^{2+} reflect both the Hg:MT stoichiometry and the coordination geometry around the Hg^{2+}. The CD spectral data shown in Figures 2, 4, and 11 for apo-MT, Zn_7–MT, and Cd_7–MT unambiguously show that (i) Hg_7–MT forms as a single product with apo-MT, (ii) Hg_4–α-MT forms as a single product with apo-α-MT, (iii) Hg_{11}–MT forms at Hg:MT ratios >9 when Hg^{2+} binds to Zn_7–MT or Cd_7–MT, and (iv) the Hg_{11}–MT species is the preferred product in the presence of ethylene glycol.

(42) Jorgensen, C. K. *Prog. Inorg. Chem.* **1970**, *12*, 101–158.
(43) Hagen, K. S.; Holm, R. H. *Inorg. Chem.* **1983**, *22*, 3171–3174.

The Proposed Model. 1. The 261-nm (+) and 283-nm (–) CD bands are related to the formation of Hg_3S_9 (β) and Hg_4S_{11} (α) clusters, which involve tetrahedral coordination of Hg^{2+} in two metal thiolate domains.

2. The 303-nm (+) and 319-nm (–) CD bands that intensify when between 0 and 7 Hg^{2+} for apo-MT and between 0 and 4 Hg^{2+} for apo-α-MT arise from tetrahedral coordination of Hg^{2+} by RS^-.

3. The broad band at 301 nm that dominates the CD spectrum during the titration of Zn_7–MT with Hg^{2+} at the 10–12 Hg^{2+} point is a new band that indicates the loss of tetrahedral coordination, and the onset of formation of a new species with a structure involving 11 or 12 Hg^{2+}. From the extensive chemical and spectral data for Cu_{12}–MT[8,32,33] and Ag_{12}–MT,[34] we suggest that in this species Hg^{2+} is trigonally coordinated by cysteinyl sulfur groups. We propose that the ionic radius of Hg^{2+} is too great to stabilize the Hg_{12}–MT analogue of Cu_{12}–MT and that clusters of the type Hg_5S_9 (β) and Hg_6S_{11} (α) form rather than M_6S_9 (β) and M_6S_{11} (α) when M = Cu^+.

4. At molar ratios of Hg:MT greater than 12 and at pH > 7, a complex with an open structure forms which exhibits no CD intensity.

5. The CD intensity is a maximum for ordered metal–thiolate units of the same coordination geometry and a minimum for disordered units of mixed geometries.

Using this model as a guide, we can analyze the spectroscopic properties observed during titrations of the metallothioneins (apo-MT, apo-α-MT, Zn_7–MT, Zn_4–α-MT) with Hg^{2+}. We shall show that the 3-dimensional plots of CD spectral intensity as a function of the molar ratio of Hg:MT can be considered as "coordination landscapes" that show the formation of complexes characterized by single and highly specific coordination geometries for the mercury bound to the thiolates in metallothionein. The appearance and disappearance of spectral features over a range of Hg:MT values represent the adoption by Hg^{2+} of a single coordination geometry at that stoichiometric ratio, tetrahedral for Hg:MT = 7, trigonal for Hg:MT = 11, and linear for Hg:MT = 20. We summarize the reaction pathways identified by the CD and MCD spectral data in Figure 13 and summarize the spectral parameters in Table II.

Hg^{2+} Binding to apo-MT and apo-α-MT. Spectroscopic evidence indicates that apo-MT exists as a random coil structure[4] before addition of any metal. The growth in intensity of the 270-nm (+) CD band with up to 2 Hg^{2+} add to apo-MT (and the first Hg^{2+} added to apo-α MT) shows that only isolated $Hg(SR)_4$ units form.[17] The sharp isodichroic points that are observed, together with the saturation in the band intensities at stoichiometries of exactly 7 and 4 (for apo-α-MT), show that a single species forms, which, by comparison with Cd_7–MT, involves a tetrahedral HgS_4 geometry characterized by three bands in the CD spectrum, Table II. The CD signal characteristic of tetrahedral coordination is replaced by the characteristic trigonal signal centered on 300 nm for Hg:MT > 8 < 12. This suggests that the stability of the tetrahedral Hg_3S_9 and Hg_4S_{11} clusters inhibits formation of the trigonally based Hg_5S_9 (β) and Hg_6S_{11} (α) clusters. All CD intensity is quenched when Hg:MT > 12, which indicates that the two clusters open up with additional mercury, even though Hg–RS binding still must take place.

MCD spectral intensity is sensitive to the symmetry of coordinating groups around the metal center but is not particularly sensitive to how the amino acids are arranged around the binding site core.[17] We see two sets of MCD spectra between 1 and 7 Hg^{2+} (Figure 1). The MCD band intensity at 311 nm is very strong between 3 and 7 Hg^{2+}, resembling the A term expected for a degenerate excited state. The data provide supporting evidence that the Hg_mS_n clusters formed with $m = 3$ ($n = 9$) and

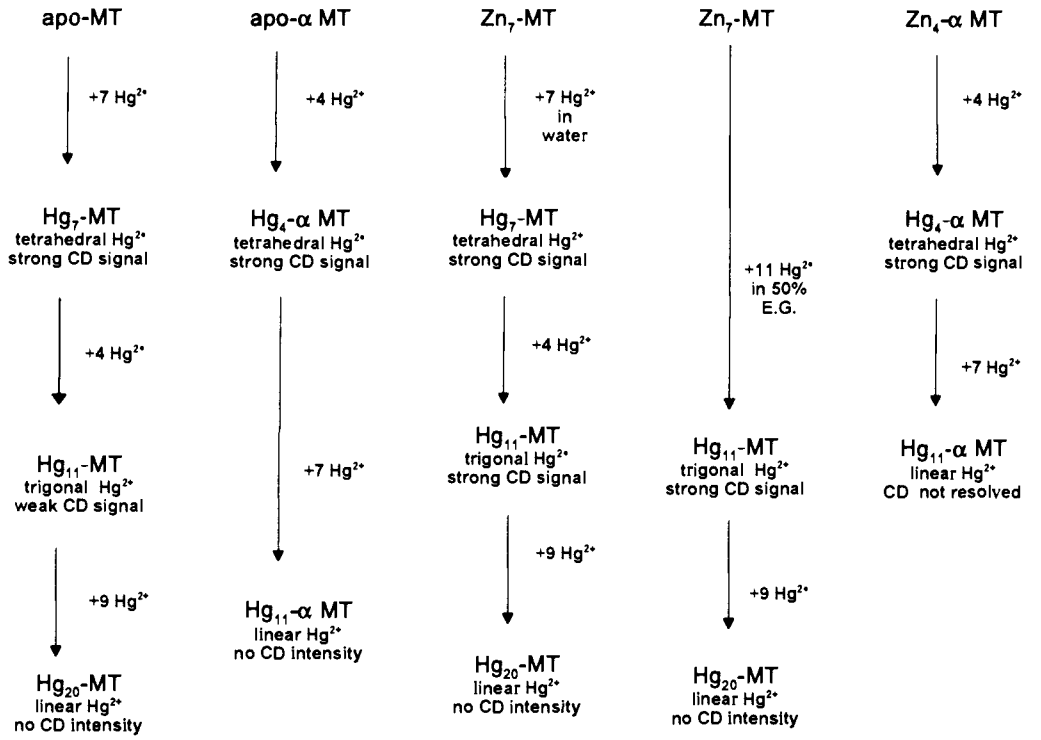

Figure 13. Species identified by distinct CD spectral envelopes following addition of Hg^{2+} to rabbit liver metallothionein.

Table II. CD and MCD Spectral Parameters for Hg-MT Species Formed by Adding Hg^{2+} to Rabbit Liver apo-MT, apo-α-MT, Zn-MT, and Zn_4-α-MT

protein used	reaction conditions[a]	species formed	band maxima and sign[b]/nm (sign)
apo-MT 2	+7 Hg^{2+}	Hg_7-MT	CD: 261 (+); 283 (-); 303 (+) MCD: 311 (-); 268 (+)
apo-α-MT 2	+4 Hg^{2+}	Hg_4-MT	CD: 261 (+); 283 (-); 300 (+); 319 (-)
Zn_7-MT 2	+7 Hg^{2+}	Hg_7-MT	CD: 262 (+); 282 (-); 297 (+) MCD: 260 (+); 311 (-)
	+11 Hg^{2+}	Hg_{11}-MT	CD: 300 (+)
Zn_4-α-MT 2	+4 Hg^{2+}	Hg_4-α-MT	CD: 260 (+); 282 (-); 300 (+); 320 (-)
Zn_7-MT	50% ethylene glycol, +11 Hg^{2+}	Hg_{11}-MT	CD: 302 (+)

[a] All reactions at 20 °C in water at pH 7, unless otherwise noted. [b] Band maxima are for CD spectra, except for MCD where noted.

$m = 4$ ($n = 11$) involve tetrahedral geometry at the mercury binding site. The collapse of the intensity following addition of >7 mol equiv of Hg^{2+} suggests the loss of the symmetric environment of the Hg^{2+}.

Hg^{2+} Binding to Zn_7-MT and Zn_4-α-MT. The spectra recorded for Zn_7-MT, Figure 4, show the presence of a new band centered on 302 nm that grows in intensity up to 11 Hg. The 240-nm Zn-(cysS)- band diminishes in intensity as a function of the stoichiometric ratio of Hg^{2+} added, as expected. The lack of the broad 270-nm marker for isolated HgS_4 units seen with apo-MT confirms that mixed Zn-(cysS)-Hg regions must form in Zn-MT, presumably with tetrahedral coordination.[15,17,30,31] The CD data suggest that Hg-(cysS)-Hg cluster formation progresses smoothly from 1 to 7 Hg^{2+} (and 1–4 with Zn_4-α-MT) and is complete with 7 Hg^{2+} (or 4). The linear growth in the intensity of the 300-nm band as a function of Hg:MT provides support that tetrahedral Hg^{2+} thiolate cluster formation involving Hg-$(cysS)_4$- units takes place from 1 to 7 Hg^{2+} and that the three bands are all connected with formation of the same cluster.

The new CD band intensity at 300 nm with Hg:MT > 9 for Zn_7-MT indicates formation of a species that we assign to a trigonally coordinated Hg_{12}-MT complex, although at present we are unable to stabilize Hg_{12}-MT and the maximum CD band intensity is measured for Hg_{11}-MT. Hg_{11}-MT is the major product at low temperatures and the sole product when 50% ethylene glycol is used as the solvent, Figure 10. We suggest that the strain in the β domain means that in place of Hg_6S_9, Hg_5S_9 forms together with Hg_6S_{11} (α). Trigonal geometry for thiolate coordination of mercury has been recently reported for alphatic thiolates[44-46] and also for the Hg-MerR metalloregulatory protein.[47]

Temperature and Solvent Effects. We suggest that CD bands at 261 (+), 283 (-), and 300 nm are related to cluster formation with tetrahedral HgS_4, whereas the isolated 300-nm band is assigned to trigonal HgS_3 formation. At 5 °C, the lack of intensity in the HgS_4 bands shows that the trigonal complex dominates as in ethylene glycol, with a band maximum occurring at Hg:MT of 9, although the contour diagram in Figure 7 shows that Hg^{2+} binds up to the 11 point before the domains collapse as at higher temperatures. Observation of a maximum at Hg:MT = 9 does not imply that Hg_9-MT forms, just that complete expression of the Hg_{11}-MT structure is inhibited at low temperatures. The resolution between the tetrahedrally based Hg_7-MT and the trigonally based Hg_{11}-MT is emphasized at 50 °C, Figure 8. We associate the loss of all characteristic spectral properties at 70 °C (Figure 9) with a general thermodynamic destabilization of large cluster complexes.

Hg^{2+} Binding to Cd_7-MT and Cd_4-α-MT. The CD data presented here very clearly show that cadmium completely inhibits formation of Hg_7-MT in which Hg^{2+} is tetrahedrally coordinated by sulfur. In addition, Hg_{11}-MT formation is also strongly inhibited. The CD data in Figure 11 clearly show that Hg^{2+} binding to Cd_7-MT is much more complicated than that with

(44) Hencher, J. L.; Khan, M.; Said, F. F.; Tuck, D. G. *Polyhedron* **1985**, *4*, 1261–1267.
(45) Watton, S. P.; Wright, J. G.; MacDonnell, F. M.; Bryson, J. W.; Sabat, M.; O'Halloran, T. V. *J. Am. Chem. Soc.* **1990**, *112*, 2824–2826.
(46) Gruff, E. S.; Koch, S. A. *J. Am. Chem. Soc.* **1990**, *112*, 1245–1247.
(47) Wright, J. G.; Tsang, H. T.; Penner-Hahn, J. E.; O'Halloran, T. V. *J. Am. Chem. Soc.* **1990**, *112*, 2434–2435.

apo-MT or Zn_7–MT. It is not surprising that analysis of the absorption spectra recorded for different ratios of Cd;Hg;MT required a number of unique species.[26] Analysis of the CD spectra shows that no single species dominates the speciation.

The derivative-shaped CD signal of Cd_7–MT, which is due to the presence of the Cd_4S_{11} cluster in the α domain,[17,18] is quenched as expected when 7 Hg^{2+} have been added. The lack of a distinct Hg_7–MT spectrum of the type recorded for titrations with apo-MT and Zn_7–MT suggests that Hg^{2+} binding to Cd_7–MT follows a "distributed" manner, that is, Hg^{2+} binds statistically in both α and β domains. If Hg^{2+} binding to Cd_7–MT were "domain specific" into the α domain first, we should see the derivative-shaped CD signal characteristic of Cd_7–MT collapse at the 4 Hg^{2+} point rather than with 7 Hg^{2+}. We propose that this is probably because the Hg_mS_n domains involve a mixture of coordination geometries, possibly not only tetrahedral and linear coordinated mercury as described by Johnson and Armitage[26] but also trigonal coordination.[44-47] The effect of the Cd^{2+} is even more pronounced when Hg^{2+} is added to Cd_4–α-MT. The more resolved CD spectrum of Cd_4–α-MT[17] suggests a tighter structure than in Cd_7–MT, and we interpret the spectral changes reported here as indicating that no well-defined mercury thiolate structure forms.

Conclusions

1. We propose that the coordination geometry around mercury bound to metallothionein can be tetrahedral (in Hg_7–MT), trigonal (in Hg_1 MT), or linear (in Hg_{20}–MT).

2. Hg_7–MT and Hg_4–α-MT form solely during titrations of apo-MT with Hg^{2+} at pH > 7, which from analysis of XANES data[29] and by comparison with the spectral and structural data reported for Cd_7–MT[15,17,31] is compelling evidence that distinct Hg_4S_{11} clusters form in the α domain and Hg_3S_9 clusters form in the β domain and that both involve tetrahedral coordination of the Hg^{2+} by sulfur. There is *no indication of mixed coordination geometries when Hg–MT forms from apo-MT.*

3. Titration of Zn_7–MT with Hg^{2+} results in formation first of Hg_7–MT, with tetrahedral coordination, and second of Hg_{11}–MT, a species that is characterized as involving trigonal coordination.

4. The trigonal Hg_{11}–MT species is the only product when the titration of Zn_7–MT is carried out in 50% ethylene glycol. This trigonal complex is also the preferred product when titrations of Zn_7–MT are carried out at 5 °C.

5. Multiple species associated with different coordination geometries are present at molar ratios between 1 and 12 Hg:MT when Hg^{2+} is added to Cd_7–MT.

6. Addition of further mercury at pH > 7 to apo-MT, Zn–MT, or Cd–MT opens up the complexes that have formed and quenches the CD spectral intensity. This is unlike the behavior observed for cadmium binding and suggests that a Hg_{20}–MT species exists which involves a random coil with linear X-Hg-(cysS)- binding (X = counterion).

Acknowledgment. This work was supported by the Natural Sciences and Engineering Research Council of Canada under the Operating and Strategic Grants program. We wish to acknowledge the support of the Centre for Chemical Physics at the University of Western Ontario. We wish to acknowledge preliminary experiments carried out by Drs. Annie Law and Jadwiga Szymanska. This is publication number 486 of the Photochemistry Unit at the University of Western Ontario.